Biochemical and Biophysical Research Communications 462 (2015) 358–364

Contents lists available at ScienceDirect

Biochemical and Biophysical Research Communications

journal homepage: www.elsevier.com/locate/ybbrc

The A- and B-type muscarinic acetylcholine receptors from *Drosophila melanogaster* couple to different second messenger pathways

Guilin R. Ren, Jonas Folke, Frank Hauser, Shizhong Li, Cornelis J.P. Grimmelikhuijzen*, [1]

Center for Functional and Comparative Insect Genomics, Department of Biology, University of Copenhagen, Universitetsparken 15, DK-2100 Copenhagen, Denmark

ARTICLE INFO

Article history:
Received 29 April 2015
Available online 9 May 2015

Keywords:
G protein-coupled receptor
GPCR
Acetylcholine
Hormone
Signaling
Insect

ABSTRACT

Muscarinic acetylcholine receptors (mAChRs) are G protein-coupled receptors (GPCRs) that are activated by the agonists acetylcholine and muscarine and blocked by several antagonists, among them atropine. In mammals five mAChRs (m1-m5) exist of which m1, m3, and m5 are coupled to members of the $G_{q/11}$ family and m2 and m4 to members of the $G_{i/0}$ family. We have recently shown that *Drosophila melanogaster* and other arthropods have two mAChRs, named A and B, where the A-type has the same pharmacology as the mammalian mAChRs, while the B-type has a very low affinity to muscarine and no affinity to classical antagonists such as atropine. Here, we find that the *D. melanogaster* A-type mAChR is coupled to $G_{q/11}$ and *D. melanogaster* B-type mAChR to $G_{i/0}$. Furthermore, by comparing the second and third intracellular loops of all animal mAChRs for which the G protein coupling has been established, we could identify several amino acid residues likely to be specific for either $G_{q/11}$ or $G_{i/0}$ coupling. Using these hallmarks for specific mAChR G protein interaction we found that all protostomes with a sequenced genome have one mAChR coupled to $G_{q/11}$ and one to four mAChRs coupled to $G_{i/0}$. Furthermore, in protostomes, probably all A-type mAChRs are coupled to $G_{q/11}$ and all B-type mAChRs to $G_{0/i}$.

1. Introduction

Acetylcholine was the first neurotransmitter to be identified [1] and is still one of the most thoroughly studied transmitters. Acetylcholine signaling occurs through the fast ionotropic nicotinic acetylcholine receptors (nAChRs), or the more slowly acting metabotropic muscarinic acetylcholine receptors (mAChRs) [2,3]. Mammals have five mAChRs (m1-m5), of which m1, m3, and m5 are coupled to members of the $G_{q/11}$ family, leading to activation of phospholipase C-beta and an intracellular IP_3/Ca^{2+} cascade, which is mostly excitatory. Two other mAChRs (m2 and m4) are coupled to members of the $G_{i/0}$ family, which either lead to an inhibition (mediated by $\alpha_{i/0}$) of adenylate cyclase resulting in a decrease of intracellular cAMP, or to the opening of a G protein-coupled potassium channel (GIRK), mediated by the $\beta\gamma$ subunit of $G_{i/0}$. The results of $G_{i/0}$ activation are, in both cases, inhibition or hyperpolarisation of the target cells [2,3].

In mammals, the mAChRs play a central role in the parasympathetic nervous system, where they activate (m1, m3, m5) or inhibit (m2, m4) target organs in the periphery [2,3]. mAChRs are also widely expressed in the central nervous system, where they play a role in learning, memory, and reward and, therefore, also in the diseases associated with these processes, such as Alzheimer's disease and drug addiction [2–4].

Most multicellular animals belong to two evolutionary lineages, the Protostomia, such as insects and most other invertebrates, and the Deuterostomia, such as vertebrates and mammals (Fig. 1). We have recently found that *Drosophila melanogaster* and other insects have two types of mAChRs, named A and B. The A-type mAChRs are pharmacologically very similar to the mammalian m1-m5 receptors, being activated by the agonists acetylcholine and muscarine and inhibited by the antagonists atropine, 3-quinuclidinyl-benzilate (QNB), and scopolamine [5]. The B-type mAChRs, however, have a pharmacology that is quite different from the mammalian mAChRs. They have a high sensitivity to acetylcholine, but a 1000-fold lower sensitivity to muscarine than the A-type receptors and are not blocked by the classical antagonists [5].

The crystal structures of the human m2 and rat m3 receptors bound to their antagonists have recently been determined,

* Corresponding author.
E-mail address: cgrimmelikhuijzen@bio.ku.dk (C.J.P. Grimmelikhuijzen).
[1] URL: http://www2.bio.ku.dk/insect_genomics/members/Cornelis_Grimmelikhuijzen/.

http://dx.doi.org/10.1016/j.bbrc.2015.04.141
0006-291X/

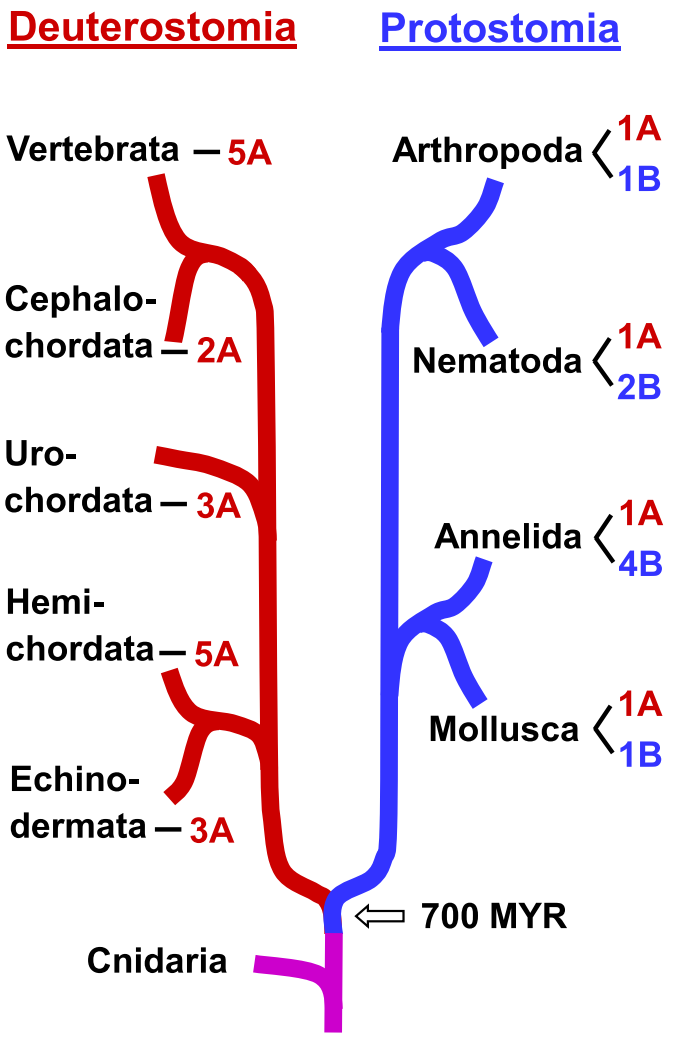

Fig. 1. Simplified phylogenetic tree of multicellular animals, showing the proto- and deuterostome evolutionary lines (highlighted in blue and red) and the emergence of A- and B-type mAChRs. Cnidarians evolved before the split of proto- and deuterostomes (highlighted in purple). Modified from Ref. [5].

including the positions of 14 amino acid residues that form the binding pocket for the classical mAChR antagonists QNB and tiotropium [6,7]. An alignment of the *D. melanogaster* A-type mAChR with the human m2 and rat m3 receptors showed that its antagonist binding pocket is identical to those from the mammalian receptors, demonstrating that the insect A-type mAChRs are not only pharmacologically, but also structurally very similar to the mammalian mAChRs [5]. A similar alignment of the *D. melanogaster* B-type mAChR with the mammalian mAChRs, however, showed that many residues forming the antagonist binding pockets in the mammalian receptors are quite different from those forming the corresponding binding pocket in the *D. melanogaster* B-type receptors [5]. These results, then, give a structural explanation for the lack of sensitivity of the B-type receptors to the classical antagonists atropine, QNB, and scopolamine.

We previously characterized the A- and B-type receptors from *D. melanogaster* using Chinese Hamster Ovary (CHO) cells transfected with the promiscuous G protein G_{16} [5]. This G protein initiates an IP_3/Ca^{2+} second messenger cascade independent from whether the GPCR normally couples to $G_{q/11}$, G_s, or $G_{i/0}$ [8]. An important question that remains, therefore, is to which second messenger pathways these *D. melanogaster* receptors normally couple. This question is addressed in the current paper, where we find that the A-type mAChR couples to the $G_{q/11}$ and the B-type to the $G_{i/0}$ pathways. Furthermore, we propose hallmarks in mAChRs specific for either $G_{q/11}$ or $G_{i/0}$ coupling.

2. Materials and methods

2.1. Cell culture, transfection, and bioassays

The CHO–K1 cells, stably expressing G_{16} and human embryonic kidney (HEK-293) cells stably expressing cyclic nucleotide gated (CNG) ion channels have previously been described [5,8–12]. DNAs coding for the short splicing variants of A- or B-type *D. melanogaster* mAChRs were used for all transfections [5].

The bioassays for measuring intracellular Ca^{2+} concentrations using aequorin bioluminescence were carried out as in Refs. [5,8–12]. HEK cells, in contrast to CHO cells, express endogenous m1 mAChRs, To minimize interference from these mAChRs, HEK-CNG cells were preincubated with 75 μM chloroquine 1.5 h prior to the bioassays to block the IP_3 receptor [13]. To obtain maximal concentrations of intracellular cAMP, the adenylate cyclase activator forskolin (final concentration 1 μM) and the phosphodiesterase inhibitor 3-isobutyl-1-methylxantine (IBMX) (final concentration 100 μM) were added 5 min prior to the assay. All cells shown within one panel in Fig. 2 or Fig. 3 were measured at the same time. All bioassays were measured as three biological replicates ($n = 3$) and were repeated at least five times.

2.2. Accession numbers, data analyses, and software

Protein sequence alignments were carried out using ClustalW2 (http://www.ebi.ac.uk/Tools/msa/clustalw2/). The protein sequences given in Fig. 4 can be retrieved using the following NCBI Accession Nos. Ac-A (*Aplysia californica*) XP_005107677; Ac–B (*A. californica*) XP_005113431; Am-A (*Apis mellifera*) XP_006608645; Am–B (*A. mellifera*) XP_006558421; Cg-A (*Crassostrea gigas*) XP_011425897; Cg-B (*C. gigas*) XP_011443835; Dm-A (*D. melanogaster*) AFJ23965; Dm-B (*D. melanogaster*) AGE13748; GAR-1 (*Caenorhabditis elegans*) AAD13747; GAR-2 (*C. elegans*) AAL15153; GAR-3 (*C. elegans*) AAD48771; Hr-A (*Helobdella robusta*) XP_009008924; Hr-B1(*Helobdella robusta*) XP_009013490; Hr-B2 (*Helobdella robusta*) annotated from scaffold AMQM01008244, merge of partial sequences XP_009031019 and XP_009031020; Hr-B3 (*Helobdella robusta*) annotated from scaffold AMQM01000097, merge of partial sequences XP_009008904 and XP_009008905; Hr-B4 (*Helobdella robusta*) annotated from scaffold AMQM01001291, merge of partial sequences XP_009008904 and XP_009025320; Hs-M1 (*Homo sapiens*) NP_000729; Hs-M2 (*H. sapiens*) NP_000730; Hs-M3 (*H. sapiens*) NP_000731; Hs-M4 (*H. sapiens*) NP_000732; Hs-M5 (*H. sapiens*) NP_036257; Tc-A (*Tribolium castaneum*) AGG09676; Tc–B (*T. castaneum*) AFJ23967. Dose-response curves were created using GraphPad Prism (GraphPad Software V5.0). The EC_{50} or IC_{50} values were ±standard error of the mean (S.E.M), $n = 3$. The unpaired student-t test was used for statistical analysis. **, $P \leq 0.01$; ***, $P \leq 0.001$.

3. Results

3.1. The D. melanogaster A-type mAChR is coupled to the $G_{q/11}$ pathway

We have previously found that CHO cells that were stably transfected with DNA coding for G_{16} and *D. melanogaster* A-Type mAChR produce functional mAChRs initiating the IP_3/Ca^{2+} second messenger pathway [5]. However, whether this was due to an interaction of the A-type mAChR with G_{16} or $G_{q/11}$ remained unclear,

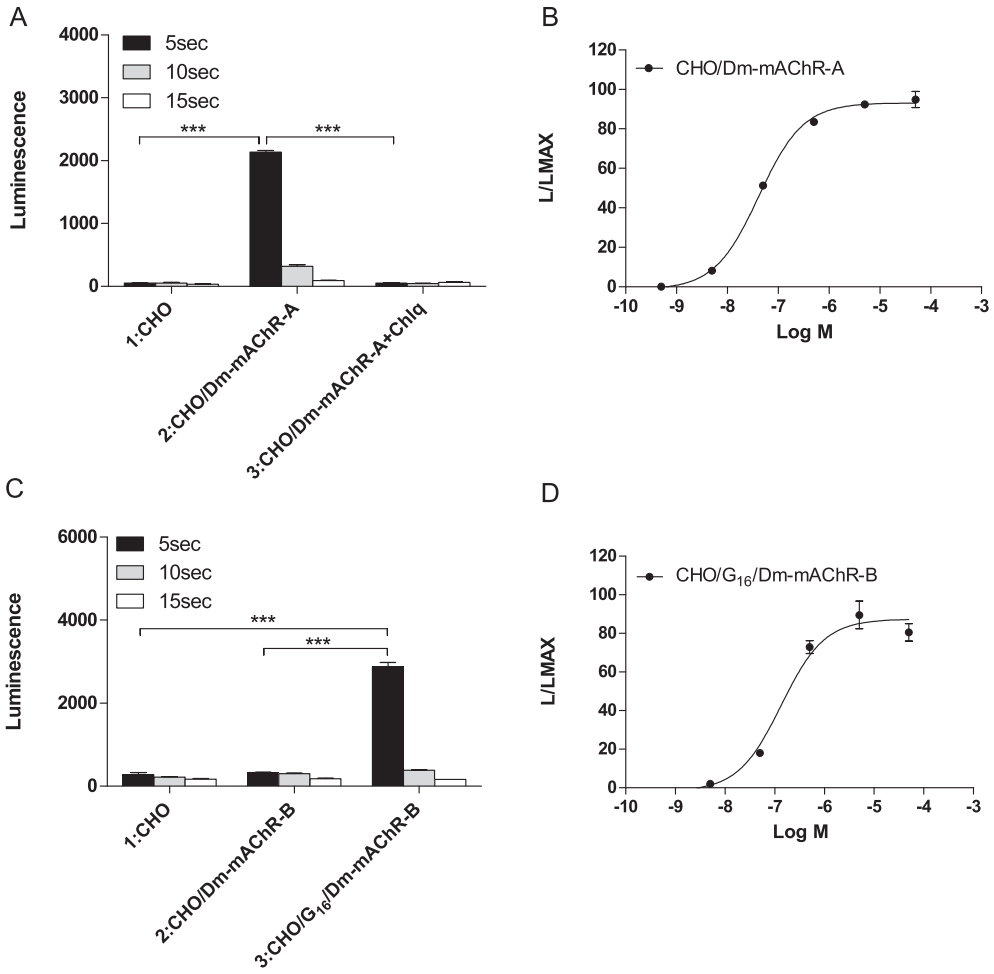

Fig. 2. Bioluminescence responses of CHO cells stably transfected with DNA coding for *D. melanogaster* A- or B-type mAChRs or empty pIRES transfection vector (=CHO). The vertical bars represent S.E.M. (n = 3), which are sometimes smaller than the symbols used. In these cases, only the symbols are given. The unpaired student-t test was used for statistical analyses; ***, $P \leq 0.001$. Log M written at the abscissae means log (acetylcholine concentrations) given in M. L/LMAX written at the ordinates means luminescence divided by maximal luminescence. (A) After addition of 10^{-6} M acetylcholine, the control CHO cells (columns 1) do not respond, while the cells transfected with DNA coding for the *D. melanogaster* A-type mAChRs (columns 2) show a strong response within the first 5 s after addition of acetylcholine. This strong response of the cells containing the A-type mAChRs is blocked by the IP_3 receptor blocker chloroquine (75 μM) (columns 3). The P values are P = 0.0000002 for the differences between column 1 and 2, and P = 0.0000002 for the differences between column 2 and 3. (B) A dose–response curve of the bioluminescence induced by acetylcholine in *D. melanogaster* A-type mAChR cells. The EC_{50} is 8×10^{-8} M. (C) No response after addition of 10^{-6} M acetylcholine to the control cells (columns 1); no response in CHO cells stably transfected with DNA coding for the *D. melanogaster* B-type mAChR (columns 2). However, a strong response after addition of 10^{-6} M acetylcholine to CHO cells that were stably transfected with both DNA coding for G_{16} and DNA coding for *D. melanogaster* B-type mAChR (columns 3). The P values are P = 0.00002 for the differences between column 1 and column 3, and P = 0.00003 for the differences between column 2 and column 3. (D) A dose response curve of the bioluminescence induced by acetylcholine in cells permanently transfected by DNA coding for G_{16} and DNA coding for *D. melanogaster* B-type mAChR. The EC_{50} is 4×10^{-7} M.

because both G_{16} or $G_{q/11}$ stimulate phospholipase C-beta, leading to the IP_3/Ca^{2+} cascade. We, therefore, stably transfected CHO cells not expressing G_{16} with DNA coding for the *D. melanogaster* A-type mAChR and found that also these cells reacted with a bioluminescence response to the addition of 10^{-6} M acetylcholine (Fig. 2A, columns 2). The responses of these cells could be blocked by the IP_3 receptor blocker chloroquine [13], showing that they are dependent on the intracellular IP_3/Ca^{2+} pathway (Fig. 2A, columns 3). Cells that were not transfected with *D. melanogaster* A-type mAChR DNA did not show a response to acetylcholine (Fig. 2A, columns 1). These data together strongly suggest that the *D. melanogaster* A-Type mAChRs are coupled to $G_{q/11}$.

Fig. 2B shows the dose–response curve of the bioluminescence induced by acetylcholine in *D. melanogaster* A-type mAChR expressing CHO cells. This dose–response curve yields an EC_{50} of 8×10^{-8} M, which is similar to the EC_{50} values found earlier for CHO cells that were stably transfected by both G_{16} and *D. melanogaster* A-type mAChR DNAs [5].

3.2. The *D. melanogaster* B-type mAChR is not coupled to the $G_{q/11}$ pathway

A similar experiment for the *D. melanogaster* B-type mAChR shows that CHO cells transfected with DNA coding for this receptor can not be activated by acetylcholine (Fig. 2C, columns 2). Only CHO cells stably cotransfected with DNAs coding for G_{16} and *D. melanogaster* B-type mAChR produce a bioluminescence response after the addition of 10^{-6} M acetylcholine (Fig. 2C, columns 3). The EC_{50} of this effect is 4×10^{-7} M (Fig. 2D), which is similar to what we found earlier for the B-type receptors [5].

3.3. The *D. melanogaster* B-type mAChR is coupled to the $G_{i/0}$ pathway

We used HEK cells stably transfected with DNA coding for cyclic nucleotide-gated (CNG) ion channels [12] to investigate whether the *D. melanogaster* B-type mAChR is coupled to the cAMP second

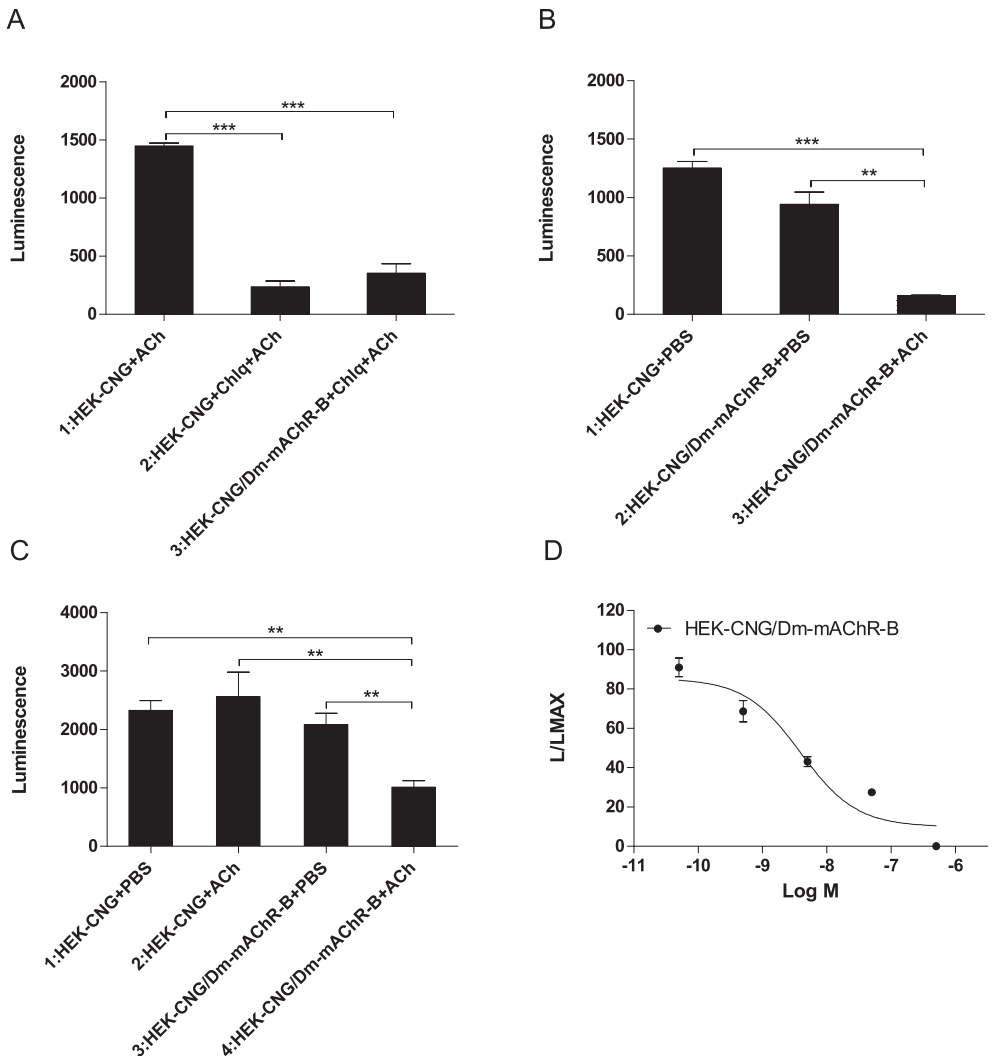

Fig. 3. Bioluminescence responses of HEK cells stably transfected with DNA coding for cyclic nucleotide-gated (CNG) channels (HEK-CNG) and transiently transfected with DNAs coding for either the *D. melanogaster* B-type mAChR or the empty pIRES transfection vector. The responses 5 s after addition of 10^{-6} M acetylcholine are shown. The statistics were carried out as in Fig. 2. Also Log M and L/LMAX are described in the legend of Fig. 2. Chlq means chloroquine. (A) Addition of 10^{-6} M acetylcholine to control HEK-CNG cells yields a bioluminescence response (column 1), which is probably due to the endogenous m1 receptor [15]. This response can be blocked by the IP_3 receptor blocker chloroquine (column 2), showing that the bioluminescence response uses the IP_3/Ca^{2+} pathway. A similar blocked response can be seen when HEK-CNG cells are transiently transfected with DNA coding for *D. melanogaster* B-type mAChR (column 3). The P values are P = 0.00003 for the differences between column 1 and column 2, and P = 0.0002 for the differences between column 1 and column 3. (B) All cells shown in this figure were pretreated with 75 μM chloroquine 2 h before the assay to block the bioluminescence response caused by the endogenous m1 mAChRs as shown in Fig. 3A. Furthermore, all cells were pretreated with 1 μM forskolin and 100 μM IBMX 5 min before start of the assay. HEK-CNG control cells pretreated in this way show a strong bioluminescence (column 1). This activity is probably caused by an increase in intracellular cAMP, which opens the CNG channels, thereby allowing Ca^{2+} influx from the extracellular medium [12,14]. A similar bioluminescence is seen after forskolin and IBMX pretreatment of HEK-CNG cells transiently transfected with DNA coding for the *D. melanogaster* B-type mAChR (column 2). When 10^{-6} M acetylcholine is added to these HEK-CNG cells expressing the *D. melanogaster* B-type mAChRs, the bioluminescence is strongly diminished (column 3). This decrease is probably due to lowered intracellular cAMP concentrations. We, therefore, conclude that activated *D. melanogaster* B-type mAChRs couple to $G_{i/0}$ leading to inhibition of adenylate cyclase. The P values are P = 0.0004 for the differences between column 1 and column 3, and P = 0.002 for the differences between column 2 and column 3. (C) A similar experiment as in Fig. 3B showing that control HEK-CNG cells pretreated with forskolin and IBMX display bioluminescence (column 1). This bioluminescence does not decrease after addition of 10^{-6} M acetylcholine (column 2), showing that there is no endogenous mAChR coupling to ($G_{i/0}$). Columns 3 and 4 show a similar experiment as in Fig. 3B, columns 2 and 3. The P values are P = 0.003 for the differences between column 1 and column 4, P = 0.009 for the differences between column 2 and column 4, and P = 0.009 for the differences between column 3 and column 4. (D) A dose response curve of the acetylcholine-induced inhibition of the bioluminescence seen in Fig. 3B, column 3. The IC_{50} is 4 x 10^{-9} M.

messenger pathways. When cAMP concentrations rise in these cells, the CNG channels are opened, allowing extracellular Ca^{2+} (and Na^{+}) to enter the cell, resulting in a bioluminescence response [12,14]. However, HEK cells express an endogenous m1 mAChRs [15], meaning that when acetylcholine is added, these cells start an IP3/$Ca2^{+}$ second messenger cascade and display a bioluminescence response (Fig. 3A, column 1). This bioluminescence response can be blocked by the IP_3 receptor blocker chloroquinine, confirming that the effect is mediated by $G_{q/11}$ and the IP_3/Ca^{2+} pathway (Fig. 3A, column 2). Also when HEK-CNG cells are transiently transfected by DNA coding for *D. melanogaster* B-type mAChR, the bioluminescence response to acetylcholine remains blocked by chloroquine (Fig. 3A, column 3). This result means that the B-type mAChR can not activate adenylate cyclase via G_s, which would increase the intracellular cAMP and open the CNG channels, thereby allowing extracellular Ca^{2+} to enter the cell and give a bioluminescence signal.

HEK-CNG cells pretreated with chloroquine (to block the IP_3/Ca^{2+} pathway) and forskolin plus 3-isobutyl-1-methylxanthine (IBMX) (to increase the intracellular cAMP concentrations by

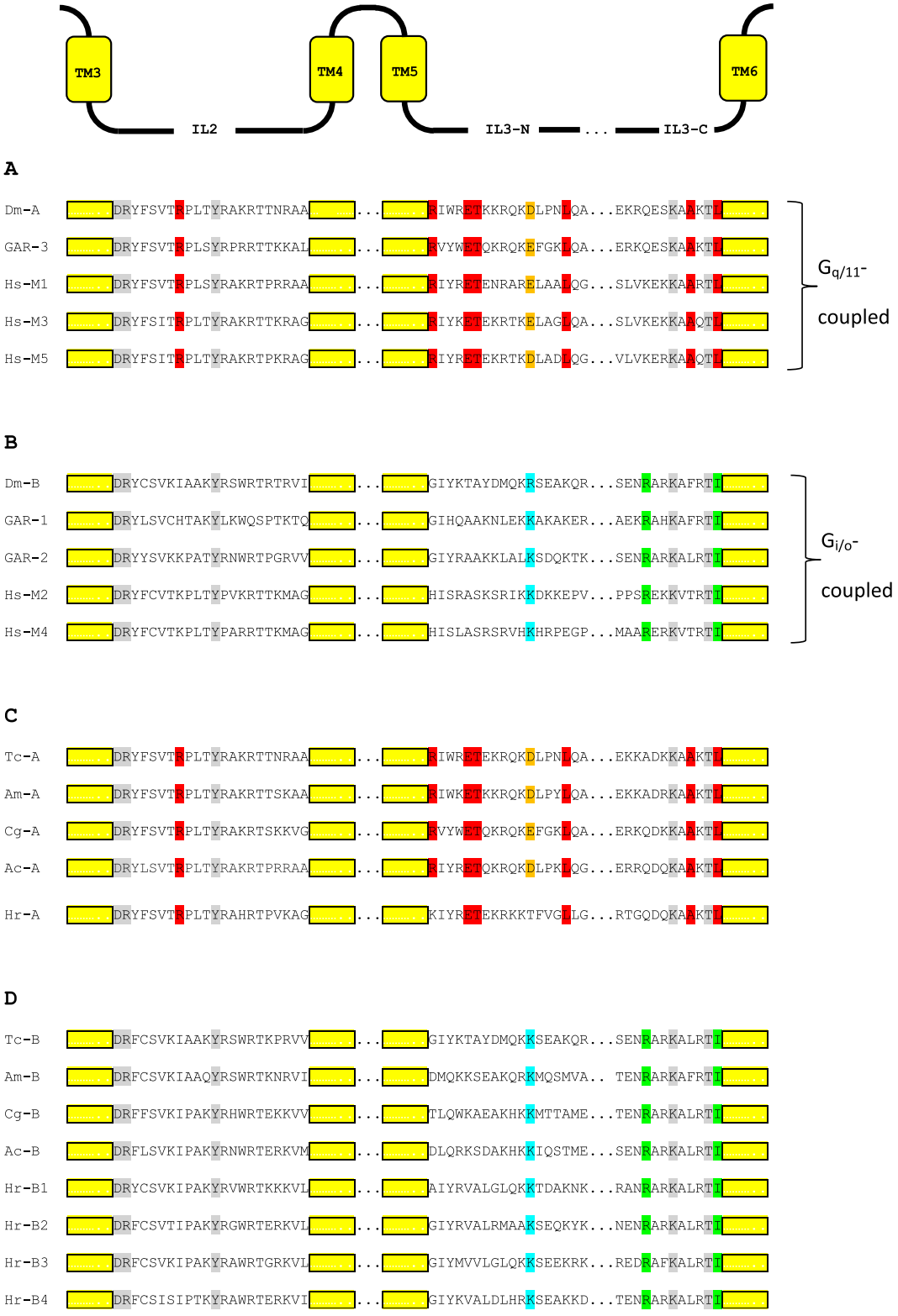

Fig. 4. Alignments of the second (IL2) and third (IL3) intracellular loops of several mAChRs from animal species with a sequenced genome. For the protostomes we have selected at least one species from the various phyla or subphyla shown in Fig. 1. Dm-A and -B = *D. melanogaster* A- and B-type mAChRs [5]; GAR-1, -2, -3 = *C. elegans* (nematode) mAChR -1, -2, -3 [16–18]; Hs-m1 to -m5 = *Homo sapiens* m1–m5 receptors [2,3]; Tc-A and -B = *Tribolium castaneum* (arthropod) A- and B-type mAChRs [5]; Am-A and -B = *Apis mellifera* (arthropod) A- and B-type mAChRs; Cq-A and -B *Crassostrea gigas* (mollusc) A- and B-type mAChRs; Ac-A and -B = *Aplysia california* (mollusc) A- and B-type mAChRs; Hr-A and -B = *Helobdella robusta* (annelid) A- and B-type mAChRs. Amino acid residues that are identical in all mAChRs are highlighted in grey. (A) It appears that all mAChRs known to be coupled to $G_{q/11}$ have several identical amino acid residues in common (highlighted in red), which are absent in the mAChRs known to be coupled to $G_{i/0}$ (Fig. 4B). The residues highlighted in orange are acidic (not identical but conserved) amino acid residues, which are basic residues at corresponding positions in the $G_{i/0}$-coupled receptors (Fig. 4B). (B) Similarly, the mAChRs known to be coupled to $G_{i/0}$ also have common identical residues (highlighted in green) that are absent in the $G_{q/11}$-coupled mAChRs (Fig. 4A). The residues highlighted in blue are basic (not identical but conserved) amino acid residues that are acidic residues at corresponding positions in $G_{q/11}$-coupled receptors (Fig. 4A). (C) mAChRs that can be assigned as A-type [5] (see Fig. 1) have the same hallmarks as the $G_{q/11}$-coupled receptors from Fig. 4A. The annelids (Hr-A), however, have a few minor deviations. (D) mAChRs that can be assigned as B-type [5] (see Fig. 1) have the same hallmarks as the $G_{i/0}$-coupled receptors from Fig. 4B, which is also true for the annelids (Hr-B1 to Hr-B4).

stimulating adenylate cyclase and blocking phosphodiesterase) displayed a strong bioluminescence response (Fig. 3B, column 1). The same phenomenon is seen in HEK-CNG cells transiently transfeceted with DNA coding for the *D. melanogaster* B-type mAChR (Fig. 3B column 2). However, when 10^{-6} M acetylcholine is added to these HEK-CNG/B-mAChR cells, most of the bioluminescence disappears (Fig. 3B, column 3). These results demonstrate that the *D. melanogaster* B-type mAChR couples to $G_{i/0}$, which inhibits the production of cAMP.

Control HEK-CNG cells, pretreated with chloroquine, forskolin, and IBMX as above (Fig. 3C, column 1) do not diminish their bioluminescence after the addition of 10^{-6} M acetylcholine (Fig. 3C, column 2), showing that these control cells do not have endogenous mAChRs coupled to $G_{i/0}$.

Fig. 3D shows the dose–response curve of the acetylcholine effect given in Fig. 3B (column 3). The IC_{50} for acetylcholine is 4×10^{-9} M, which is considerably lower than the EC_{50} for acetylcholine activating the *D. melanogaster* A-type mAChR (8×10^{-8} M, see Fig. 2B). Remarkably, it is even two orders of magnitude lower than the EC_{50} for acetylcholine activating the B-type mAChR in CHO-G_{16} cells (4×10^{-7} M, see Fig. 2D).

3.4. Hallmarks in the amino acid sequences of the intracellular loops of mAChRs predict coupling to $G_{q/11}$ or $G_{i/0}$

We aligned the intracellular loops of the mAChRs that are known to be coupled to $G_{q/11}$ (Fig. 4A) or $G_{i/0}$ (Fig. 4B). These alignments showed that the second and third intracellular loops of the $G_{q/11}$-coupled mAChRs contain specific amino acid residues (highlighted in red in Fig. 4A) that are not present in the corresponding loops of the $G_{i/0}$-coupled mAChRs. Likewise, the second and third intracellular loops of the $G_{i/0}$-coupled mAChRs contain specific residues (highlighted in green in Fig. 4B) that are not present in the $G_{q/11}$-coupled receptors. We assume that these specific residues are responsible for coupling the mAChRs to either $G_{q/11}$ or $G_{i/0}$. No such differences between $G_{q/11}$ and $G_{i/0}$-coupled receptors could be found in the first intracellular loops or in the intracellular C termini.

We have previously grouped the mAChRs from protostome species with a sequenced genome into A- and B-type mAChRs [5] (see also Introduction and Fig. 1). When we align these A- and B-type mAChRs, we can see that their intracellular loops have hallmarks for either $G_{q/11}$-coupling or $G_{i/0}$-coupling and that protostome A-type mAChRs always are associated with the mAChRs having $G_{q/11}$ coupling (Fig. 4C), while B-type mAChRs are associated with the mACHRs having G_i coupling (Fig. 4D). We presume, therefore, that all protostome A-type mAChRs couple to $G_{q/11}$ and all B-type mAChRs couple to $G_{i/0}$.

4. Discussion

In mammals, mAChRs have been extensively characterized, including their coupling to the various second messenger pathways [3]. For the other deuterostomes and protostomes, however, such studies have not been carried out with two exceptions: (i) In the nematode *C. elegans*, three mAChRs have been identified (GAR-1 to −3), of which one (GAR-3) couples to the $G_{q/11}$ pathway, while the other two couple to $G_{i/0}$ [16–18]; (ii) in *D. melanogaster* we find in our experiments described in the current paper that the A-type mAChRs couple to the $G_{q/11}$ and B-type mAChRs to the $G_{i/0}$ pathways (Figs. 2 and 3). The intracellular loops of GPCRs are known to be important for G protein coupling [19,20]. If we align these intracellular loops for the human, nematode, and fruitfly mAChRs, we find that the second and third intracellular loops contain residues that appear to be specific for the $G_{q/11}$-coupled mAChRs (Fig. 4A) and other residues that are specific for the $G_{i/0}$-coupled mAChRs (Fig. 4B). We assume, therefore, that these residues are important for the interactions with either $G_{q/11}$ or $G_{i/0}$.

For our hallmarks of $G_{q/11}$- or $G_{i/0}$-coupling, we have only used amino acid residues that are identical within the group of $G_{q/11}$-coupled mAChRs (highlighted in red in Fig. 4A) or $G_{i/0}$-coupled mAChRs (highlighted in green in Fig. 4B). These hallmarks, however, probably need to be expanded to also include conserved amino acid residues. As an example we have highlighted one position in orange in the $G_{q/11}$ coupled receptors (Fig. 4A) that is solely occupied by acidic residues (D and E). Interestingly, the corresponding residues in the $G_{i/0}$-coupled receptors are all basic (R and K; highlighted in blue in Fig. 4B). These two groups of conserved amino acid residues are very dissimilar, which makes them excellent markers for mAChR coupling to either $G_{q/11}$ or $G_{i/0}$, Yet, the signatures for $G_{q/11}$ and $G_{i/0}$ coupling might be more detailed than given in Fig. 4 and might even need the development of an algorithm.

We have previously grouped the protostome mAChRs in A- and B-type based on their pharmacology and structural features [5] (Fig. 1; see also Introduction). For all species with a sequenced genome we can already predict, based on these structural features, whether their mAChRs are A- or B-type, even if their pharmacology has not been determined (Fig. 1). Structurally, the *C. elegans* mAChR GAR-3 is A-type, and the GAR-1 and -2 receptors are B-type. GAR-3 and *D. melanogaster* A-type mAChRs are coupled to the $G_{q/11}$ second messenger pathway and GAR-1, GAR-2, and *D. melanogaster* B-type mAChRs to the $G_{i/0}$ pathway [5,16–18]. Would this mean that all protostome A-type mAChRs are coupled to $G_{q/11}$ and all B-type receptor to $G_{i/0}$? Accoding to Fig. 4C and D this appears to be the case.

Conflict of interest

None.

Acknowledgments

We want to thank Noah Kassem for typing the manuscript and Lundbeck Foundation for financial support.

Transparency document

Transparency document related to this article can be found online at http://dx.doi.org/10.1016/j.bbrc.2015.04.141.

References

[1] A.N. McCoy, S.Y. Tan, Otto Loewi, (1873–1961): Dreamer and Nobel laureate, Singap. Med. J. 55 (2014) 3–4.
[2] A.C. Kruse, B.K. Kobilka, D. Gautam, P.M. Sexton, A. Christopoulos, J. Wess, Muscarinic acetylcholine receptors: novel opportunities for drug development, Nat. Rev. Drug. Discov. 13 (2014) 549–560.
[3] E.C. Hulme, N.J. Birdsall, N.J. Buckley, Muscarinic receptor subtypes, Annu. Rev. Pharmacol. Toxicol. 30 (1990) 633–673.
[4] S. Jiang, Y. Li, C. Zhang, Y. Zhao, G. Bu, H. Xu, Y.W. Zhang, M1 muscarinic acetylcholine receptor in Alzheimer's disease, Neurosci. Bull. 30 (2014) 295–307.
[5] C. Collin, F. Hauser, E. Gonzalez de Valdivia, S. Li, J. Reisenberger, E.M. Carlsen, Z. Khan, N.O. Hansen, F. Puhm, L. Søndergaard, J. Niemiec, M. Heninger, G.R. Ren, C.J.P. Grimmelikhuijzen, Two types of muscarinic acetylcholine receptors in *Drosophila* and other arthropods, Cell. Mol. Life Sci. 70 (2013) 3231–3242.
[6] K. Haga, A.C. Kruse, H. Asada, T. Yurugi-Kobayashi, M. Shiroishi, C. Zhang, W.I. Weis, T. Okada, B.K. Kobilka, T. Haga, T. Kobayashi, Structure and function of the human M2 muscarinic acetylcholine receptor bound to an antagonist, Nature 482 (2012) 547–551.
[7] A.C. Kruse, J. Hu, A.C. Pan, D.H. Arlow, D.M. Rosenbaum, E. Rosemond, H.F. Green, T. Liu, P.S. Chae, R.O. Dror, D.E. Shaw, W.I. Weis, J. Wess,

B.K. Kobilka, Structure and dynamics of the M3 muscarinic acetylcholine receptor, Nature 482 (2012) 552–556.
[8] J. Stables, A. Green, F. Marshall, N. Fraser, E. Knight, M. Sautel, G. Milligan, M. Lee, S. Rees, A bioluminescent assay for agonist activity at potentially any G-protein-coupled receptor, Anal. Biochem. 252 (1997) 115–126.
[9] C. Lenz, M. Williamson, G.N. Hansen, C.J.P. Grimmelikhuijzen, Identification of four *Drosophila* allatostatins as the cognate ligands for the *Drosophila* orphan receptor DAR-2, Biochem. Biophys. Res. Commun. 286 (2001) 1117–1122.
[10] T. Secher, C. Lenz, G. Cazzamali, G. Sørensen, M. Williamson, G.N. Hansen, P. Svane, C.J.P. Grimmelikhuijzen, Molecular cloning of a functional allatostatin gut/brain receptor and an allatostatin preprohormone from the silkworm *Bombyx mori*, J. Biol. Chem. 276 (2001) 47052–47060.
[11] F. Staubli, T.J.D. Jørgensen, G. Cazzamali, M. Williamson, C. Lenz, L. Søndergaard, P. Roepstorff, C.J.P. Grimmelikhuijzen, Molecular identification of the insect adipokinetic hormone receptors, Proc. Natl. Acad. Sci. U. S. A. 99 (2002) 3446–3451.
[12] R.K. Reinscheid, J. Kim, J. Zeng, O. Civelli, High-throughput real-time monitoring of Gs-coupled receptor activation in intact cells using cyclic nucleotide-gated channels, Eur. J. Pharmacol. 478 (2003) 27–34.
[13] U.K. Misra, G. Gawdi, S.V. Pizzo, Chloroquine, quinine and quinidine inhibit calcium release from macrophage intracellular stores by blocking inositol 1,4,5-triphosphate binding to its receptor, J. Cell. Biochem. 64 (1997) 225–232.
[14] U.B. Kaupp, R. Seifert, Cyclic nucleotide-gated ion channels, Physiol. Rev. 82 (2002) 769–824.
[15] S.J. Mundell, J.L. Benovic, Selective regulation of endogenous G Protein-coupled receptors by arrestins in HEK293 cells, J. Biol. Chem. 275 (2000) 12900–12908.
[16] J.M. Hwang, D.J. Chang, U.S. Kim, Y.S. Lee, Y.S. Park, B.K. Kaang, N.J. Cho, Cloning and functional characterization of a *Caenorhabditis elegans* muscarinic acetylcholine receptor, Recept. Channels 6 (1999) 415–424.
[17] Y.S. Lee, Y.S. Park, S. Nam, S.J. Suh, J. Lee, B.K. Kaang, N.J. Cho, Characterization of GAR-2, a novel G protein-linked acetylcholine receptor from *Caenorhabditis elegans*, J. Neurochem. 75 (2000) 1800–1809.
[18] Y.S. Park, Y.S. Lee, N.J. Cho, B.K. Kaang, Alternative splicing of GAR-1, a *Caenorhabditis elegans* G-protein-linked acetylcholine receptor gene, Biochem. Biophys. Res. Commun. 268 (2000) 354–358.
[19] K.Y. Chung, Structural aspects of GPCR-G protein coupling, Toxicol. Res. 29 (2013) 149–155.
[20] S.G. Rasmussen, B.T. DeVree, Y. Zou, A.C. Kruse, K.Y. Chung, T.S. Kobilka, F.S. Thian, P.S. Chae, E. Pardon, D. Calinski, J.M. Mathiesen, S.T. Shah, J.A. Lyons, M. Caffrey, S.H. Gellman, J. Steyaert, G. Skiniotis, W.I. Weis, R.K. Sunahara, B.K. Kobilka, Crystal structure of the β2 adrenergic receptor-Gs protein complex, Nature 477 (2011) 549–555.